

The Collatz tree as an automorphism graph: a cotree density proof of the $3x + 1$ conjecture

Jan Kleinnijenhuis¹, Alissa M. Kleinnijenhuis², and Mustafa G. Aydogan³

¹Vrije Universiteit Amsterdam, The Network Institute
j.kleinnijenhuis@vu.nl

²Stanford University, Institute for Economic Policy Research
amklein@stanford.edu

³University of California San Francisco, Department of Biochemistry and Biophysics
mustafa.aydogan@ucsf.edu

June 16, 2022

Abstract

The Collatz conjecture maintains that each natural number n is a node in the Collatz tree with a root path to 1 generated by iterations of the Collatz function, which connects even n to $n/2$ and odd n to $3n + 1$. The conjecture holds if a binary subtree $T_{\geq 0}$ exists with as nodes *all* branching numbers constituting the congruence classes $[4, 16]_{18}$ with density $2/18$. For each branching number, the *upward* and *rightward* function generate arrows to two branching numbers in the directions $2n$ and $(n-1)/3$. In the automorphism graph of tree $T_{\geq 0}$, the iterates and conjugates of these two functions build outer paths from tree $T_{\geq 0}$ at its root node to two infinite sequences of nodes holding nested subtrees and disjoint cotrees. The nodes and conjugate inner arrows within each subtree and within each cotree correspond one-to-one to the nodes and arrows within tree $T_{\geq 0}$. The cumulative density of the congruence classes of numbers in disjoint cotrees of $T_{\geq 0}$ amounts to the density $2/18$ of all branching numbers, thus proving the conjecture.

The Collatz conjecture holds that iterations of the Collatz function, $C(n) = n/2$ if n is even, but $C(n) = 3n + 1$ if n is odd, reach 1 for all natural numbers n , via a finite *root path* [1] (see a few examples below).

$8 \rightarrow 4 \rightarrow 2 \rightarrow 1$ ($\rightarrow 4 \rightarrow 2 \rightarrow 1 \rightarrow \dots$)

$9 \rightarrow 28 \rightarrow 14 \rightarrow 7 \rightarrow 22 \rightarrow 11 \rightarrow 34 \rightarrow 17 \rightarrow 52 \rightarrow 26 \rightarrow 13 \rightarrow 40 \rightarrow 20 \rightarrow 10 \rightarrow 5 \rightarrow 16 \rightarrow 8 \rightarrow 4 \rightarrow 2 \rightarrow 1$

$10 \rightarrow 5 \rightarrow 16 \rightarrow 8 \rightarrow 4 \rightarrow 2 \rightarrow 1$

This simple-looking conjecture has become world-renowned after numerous attempts have demonstrated that its proof is certainly not straightforward, although the conjecture has been verified for all numbers below 2^{69} [2, 3]. In the words of Paul Erdős (1913–1996), ‘hopeless, absolutely hopeless’ [4]. Jeffrey Lagarias, the editor of a seminal book on the conjecture, illustrates that the conjecture ‘cuts across’ many different fields of mathematics.[4] The problem appeared to be ‘representative of a large class of problems concerning the behaviour under iteration of maps that are expanding on part of their domain and contracting on another part of their domain’ [4].

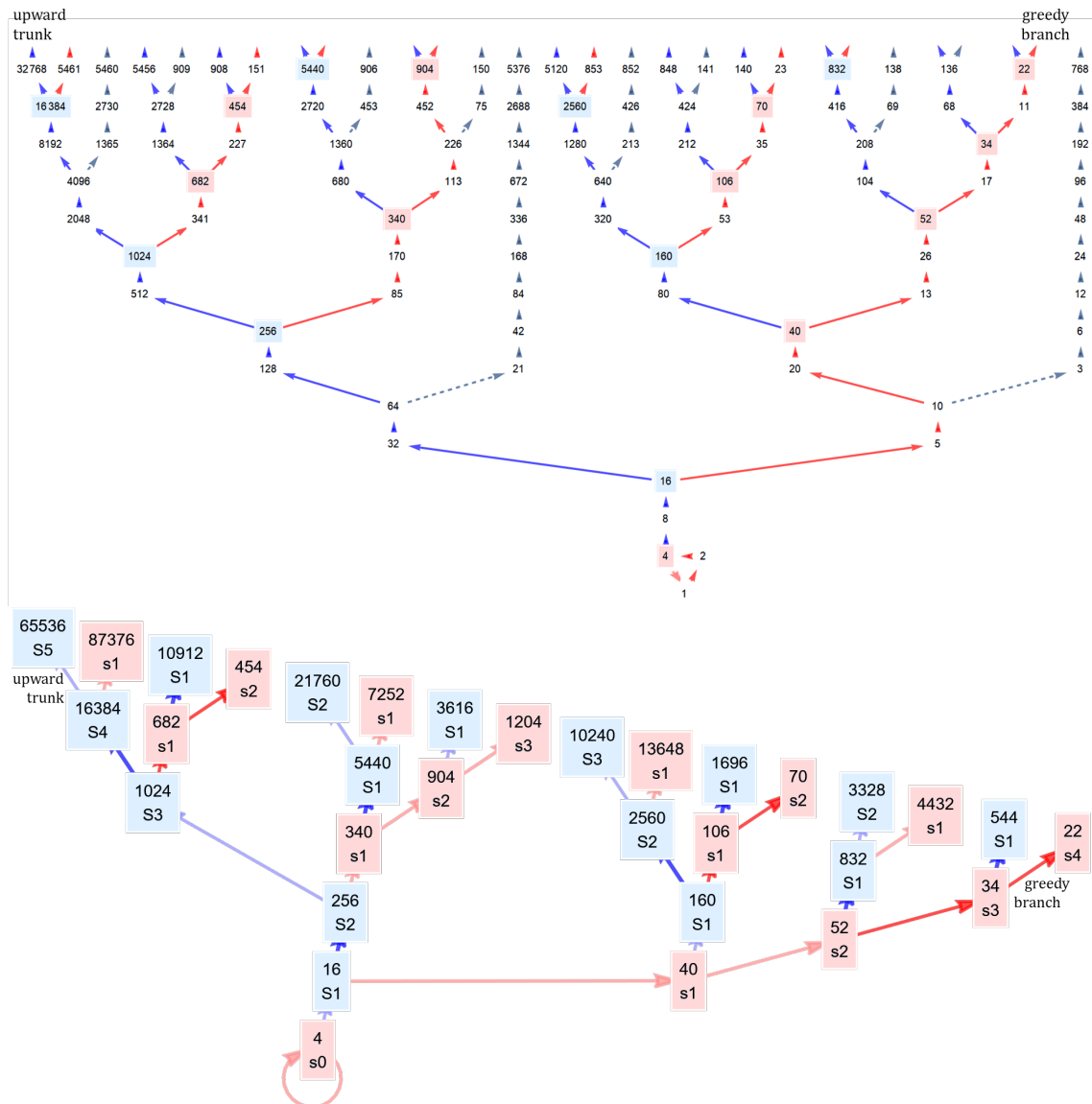


Fig. 1 | From the Collatz tree to binary tree $T_{\geq 0}$ (a) The inverse Collatz function connects branching numbers via an *upward path* of $2n$ arrows (blue) to an *upward branching number* (blue), and via a *rightward path* of an $(n-1)/3$ arrow followed by $2n$ arrows (red) to a *rightward branching number* (red). Uncoloured numbers either do not branch or do not branch to two branching successors (dashed line graphs to numbers not divisible by 3). (b) The binary tree $T_{\geq 0}$ connects branching numbers by arrows. Each rightward number (red) is the ancestor of blue-coloured upward successors $S_1 \rightarrow S_2 \rightarrow S_3 \rightarrow \dots$, e.g., $40_{s_1} \rightarrow 160_{S_1} \rightarrow 2560_{S_2} \rightarrow 10240_{S_3} \rightarrow \dots$. Each upward number (blue) is the ancestor of rightward successors $s_1 \rightarrow s_2 \rightarrow s_3 \dots$, e.g. $256_{S_2} \rightarrow 340_{s_1} \rightarrow 904_{s_2} \rightarrow 1204_{s_3} \rightarrow \dots$. The *upward trunk* (through 16384) takes just $2n$ steps. The rightward *greedy branch* (through 22) takes as many $(n-1)/3$ arrows as possible (OEIS sequence A225570) [5]. |

If the Collatz conjecture holds true, then each number n from the set of natural numbers $\mathbb{N} = 1, 2, 3, \dots$ belongs to the node set N_C of one *Collatz tree* T_C through a unique *root path* of Collatz iterations between n itself and the tree's trivial cyclic root, denoted as $\Omega_C = 1, 2, 4$. Based on tree definitions that exclude cycles, the Collatz tree should be understood as a tree with a cyclic root added.

Fig. 1a shows the Collatz tree as a *directed graph* with numbers on its lowest branches as high as 32,768, while omitting some low numbers, such as 7 and 9. Its arrows depict the *inverse* Collatz function, not with $n/2$ and $3n + 1$ but their inverses $2n$ and $(n - 1)/3$, resulting in an *upward path* of $2n$ arrows (Fig.1a, blue paths) and a *rightward path* starting with a $(n - 1)/3$ contraction and $2n$ expansions thereafter (Fig.1a, red paths). Upward and rightward children cannot be rotated, since the two inverses are *not* each other's inverses. The Collatz conjecture holds that no *isolated trajectory* exists: neither a *divergent trajectory* from n to infinity nor a *nontrivial cycle* from any $n > 4$ back to its origin n [4].

1 Proof Approach

1.1 Natural density of branching numbers

One hitherto insufficient approach to prove the Collatz conjecture, outlined by Marc Chamberland, is to find *ever less dense* node subsets $S \subset \mathbb{N}$, such that proof on S implies that it is true on \mathbb{N} [6].

Terence Tao's recent *logarithmic* density proof for 'almost all numbers' starts from the set S of odd numbers. The *Syracuse function* connects any *odd* number n directly to the next *odd* number $\text{Syr}(n)$. Its inverse $\text{Syr}^{-1}(n)$ connects n to an infinite number of successors where both n and $\text{Syr}^{-1}(n) = (2^p n - 1)/3$ are odd. For example, $n = 1$ is connected by the p -values 2, 4, 6, 8, ... *in parallel* to 1, 5, 21, 85, ..., whose $3n + 1$ map is the *serial* upward trunk $4 \rightarrow 16 \rightarrow 64 \rightarrow 256 \dots$ in the Collatz tree (Fig. 1a).[7] According to Tao, 'a full resolution of the conjecture remains well beyond current methods'.[7] The conjecture may still have exceptions or be undecidable.[7, 8, 9].

Our *natural* density proof starts from the set $S_{\geq 0}$ of (even) branching numbers with branching successors in the upward $2n$ direction and the rightward $(n - 1)/3$ direction (Fig. 1ab, blue or red). The natural density of an infinite subset S corresponding to a congruence class $[a]_m$, i.e. numbers with a residue of a after division by their periodicity or modulus m , simply amounts to $1/m$ in any successive range of m numbers (assuming $0 \leq a < m$).[10, 11] Set $S_{\geq 0}$ corresponds to the congruence classes $[4, 16]_{18}$ with density $2/18$, whose numbers branch rightward through $(n - 1)/3$ to odd congruence classes $[(4 - 1)/3, (16 - 1)/3]_{18/3} = [1, 5]_6$ (Fig.2) not divisible by 3 whose $2n$ successors can branch by $(n - 1)/3$.

The branching numbers are partitioned into generations of upward successors S_1, S_2, S_3, \dots , of rightward numbers, generations of rightward successors s_1, s_2, s_3, \dots of upward numbers and the root set s_0 of tree $T_{\geq 0}$ holding the rightward cyclic root $\Omega_{\geq 0} = 4$ (Fig.1b; Def.4).

1.2 Depict and define directed graphs

We follow Lothar Collatz (1910–1990), who specifically hoped to establish new 'connections between elementary number theory and elementary graph theory' 'using the fact that one can picture a number theoretic function $f(n)$ with a directed graph' where each iteration is with 'an arrow from n to $f(n)$ ' [1].

We depict and define a binary Collatz tree labelled $T_{\geq 0}$ (Fig.1b, Def.3) that accepts only branching numbers from set $S_{\geq 0}$, with arrows defined by the upward and rightward functions (Fig.2, Def.1, Def.2) concatenating the paths of arrows between them (Fig.1ab, red or blue)..

We also depict and define the automorphism graph of tree $T_{\geq 0}$ (Fig.5, Def.4) with trees as nodes. This graph reveals the paths along which iterates and conjugates of the upward and rightward functions map the numbers from congruence classes $[4,16]_{18}$ and arrows between them in tree $T_{\geq 0}$ one-to-one to the numbers and the arrows in two infinite series of its nested subtrees $T_{\geq 1}, T_{\geq 2}, T_{\geq 3}, \dots$ and $t_{\geq 1}, t_{\geq 2}, t_{\geq 3}, \dots$ (Fig.3) and in two infinite series of its disjoint cotrees T_1, T_2, T_3, \dots and t_1, t_2, t_3, \dots (Fig.4). The disjoint cotrees take numbers from the corresponding successor subsets S_1, S_2, S_3, \dots or s_1, s_2, s_3, \dots (Fig.4).

We prove that the cumulative density of (congruence classes of) the numbers in the disjoint cotrees of tree $T_{\geq 0}$ amounts to the density $2/18$ of all branching numbers in set $S_{\geq 0}$ (Eq. 8).

2 The upward and the rightward function

The numbers p of $2n$ arrows in Collatz paths from one branching class to the other, either without or with a preceding $(n-1)/3$ arrow, amount to congruence class contingent definitions of the upward function $U_0: n \rightarrow 2^p n$ (Def.1) and the rightward function $R_0: n \rightarrow 2^p (n-1)/3$ (Def.2). These powers p can be looked up from the directed graph in Fig. 2, which shows them as the p -values on the first $2n$ arrow (blue) in the Collatz paths connecting branching classes (purple).

Based on the upward p -vector $\vec{p}_{U_0} = [2, 4]$ of the branching argument classes $u_2 = [4, 16]_{18}$ shown in Figure 2, the upward function (Def.1) becomes $U_0(n) = [2^2 n, 2^4 n] = [4n, 16n]$, with intrinsic periodicities $[4 \cdot 18, 16 \cdot 18] = [72, 288]$. The enumeration of the output congruence classes $S_{\geq 1}$ within a least common multiple output period, requires periodicity alignment, as can be elucidated by planetary alignment or clock arithmetic. The big hand of a clock turning every 60 minutes and the small hand turning every 720 minutes yield an alignment vector $[12, 1]$, predicting $12 + 1 = 13$ different turns in 720 minutes. Similarly, the intrinsic upward output periodicities $[72, 288]$ yield the alignment vector $\vec{h}_{U_1} = [4, 1]$, resulting in five upward congruence classes $S_{\geq 1} = [[16, 88, 160, 232], [256]]_{288}$, with a least common periodicity of 288, labelled as $c5$. Set $c5$ is one of the six basic sets of congruence classes in the tree $T_{\geq 0}$ enumerated in Table 1, with set names reflecting set size. Thus, $S_{\geq 1} = [c5]_{288}$ (Def.1, Table 1), with a periodicity expansion by $\theta_{U_1} = 288/18 = 2^4$ after one iteration of U_0 . A full cycle of six $2n$ arrows appears after two iterations (Fig.2), which invariably yields $\theta_{U_2} = 2^{3 \cdot 2} = 64$ and $U_0^2(n) = 2^{3 \cdot 2} n$.

$$\text{Upward function } U_0: S_{\geq 0} \rightarrow S_{\geq 1}; n \rightarrow U_0(n) \quad (1)$$

<i>IF</i>	<i>THEN</i>						
$S_{\geq 0} u_2$	\vec{p}_U	$U_0(n)$	$S_{\geq 1}$	$=$	$[c5]_{288}$	lcm	\vec{h}_U
$[4]_{18}$	2	$4n$	$[16]_{72}$	$=$	$[16, 88, 160, 232]_{288}$	288	4
$[16]_{18}$	4	$16n$	$[256]_{288}$	$=$	$[256]_{288}$	288	1

density $\rho(S_{\geq 1}) = 5/288$;

periodicity expansions $\theta_{U_1} = 288/18 = 2^4$, $\theta_{U_2} = 2^{3 \cdot 2}$ invariably yielding $U_0^2(n) = 2^{3 \cdot 2} n$

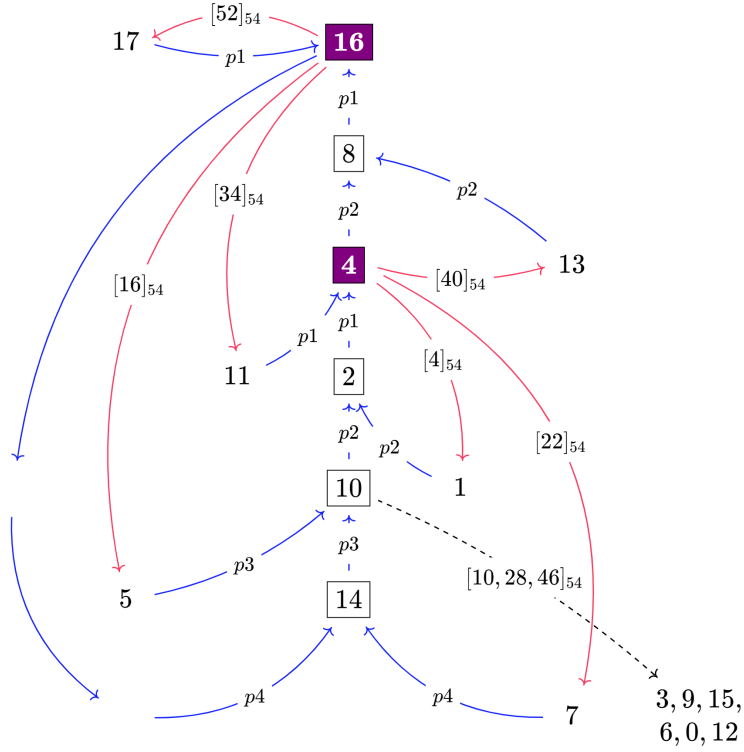


Fig. 2 | Collatz paths between branching classes. The nodes represent 18 congruence classes, modulo 18. The branching classes $[4]_{18}$ and $[16]_{18}$ (purple) are connected by a blue-only upward cycle of $2n$ arrows and six red-first rightward cycles preceded by an $(n-1)/3$ arrow to an odd class from $[1, 5, 7, 11, 13, 17]_{18}$. The label on a red $(n-1)/3$ arrow, such as $[16]_{54}$, shows which branching subclass in $r6 = [4, 16, 22, 34, 40, 52]_{54}$ with expanded periodicity $3 \cdot 18 = 54$ yields the odd class $[5]_{18}$. The p -label on the next blue $2n$ arrow, such as $5 \xrightarrow{p3}$, concatenates the path of $p = 3$ blue arrows to the next branching class $[4]_{18}$ (Fig.1a) into one $2^p = 2^3$ arrow (Fig.1b) to $[5 \cdot 2^3]_{18} = [40]_{18} = [4]_{18}$. The p -labels $\vec{p}_U = [2, 4]$ of blue-only paths starting from unexpanded classes $u2 = [4, 16]_{18}$ underpin the upward function U_0 (Def. 1). The p -labels $\vec{p}_R = [2, 3, 4, 1, 2, 1]$ of red-first paths starting from expanded branching subclasses $r6$ underpin the rightward function R_0 (Def.2). Two upward iterations yield $U_0^2(n) = 2^6 n = 64n$, either by $p2 + p4$ or $p4 + p2$. The dashed $(n-1)/3$ arrow at $[10]_{18}$ yields unbranching paths of numbers divisible by 3 (Fig.1a, dashed line graphs). |

Figure 2 also shows the p -vector $\vec{p}_R = [2, 3, 4, 1, 2, 1]$ for the six branching argument subclasses with a $3 \times$ expanded periodicity $r6 = [4, 16, 22, 34, 40, 52]_{54}$, for which $(n-1)/3$ (Fig.2, red) reaches odd classes $[1, 5, 7, 11, 13, 17]_{18}$. The rightward function (Def.2) becomes $R_0(n) = [(4, 8, 16, 2, 4, 2) \cdot (n-1)/3]$, with intrinsic periodicities $[72, 144, 288, 36, 72, 36]$. Alignment by $\vec{h}_R = [4, 2, 1, 8, 4, 8]$ yields 27 rightward congruence classes, labelled as $c27$, with a least common periodicity of 288. Figure 2 also shows that subclasses $[4, 16, 22, 34]_{54}$ connect through $[4]_{18}$ to argument subclasses $[4, 22, 40]_{54}$, while $[40, 52]_{54}$ connect through $[16]_{18}$ to $[34, 16, 52]_{54}$, yielding a $r6 \times r6$ transformation matrix T predicting for each argument class three argument classes at the next iteration.

Rightward function $R_0: S_{\geq 0} \rightarrow s_{\geq 0}; n \rightarrow U_0(n)$ (2)

<i>IF</i>		<i>THEN</i>					
$S_{\geq 0}$	$ r6$	\vec{p}_R	$R_0(n)$	$s_{\geq 0}$	$=$	$[c27]_{288}$	Lc \vec{h}_R
							m
[4] ₅₄	2	4/3 (n-1)	[4] ₇₂	=	[4, 76, 148, 220] ₂₈₈	288	4
[16] ₅₄	3	8/3 (n-1)	[40] ₁₄₄	=	[40, 184] ₂₈₈	288	2
[22] ₅₄	4	16/3 (n-1)	[112] ₂₈₈	=	[112] ₂₈₈	288	1
[34] ₅₄	1	2/3 (n-1)	[22] ₃₆	=	[22, 58, 94, 130, 166, 202, 238, 274] ₂₈₈	288	8
[40] ₅₄	2	4/3 (n-1)	[52] ₇₂	=	[52, 124, 196, 268] ₂₈₈	288	4
[52] ₅₄	1	2/3 (n-1)	[34] ₃₆	=	[34, 70, 106, 142, 178, 214, 250, 286] ₂₈₈	288	8

density $\rho(S_0) = 27/288$

periodicity expansion $\theta_R = 288/54 = 2^4 3^{-1}$, argument expansion by 3 for output expansion by $3\theta_R = 2^4$

arguments-outputs matrix T with [1,0,1,0,1,0] in rows 1-4, [0,1,0,1,0,1] in rows 5-6.

A tree is defined as a graph G with an ordered set of V (ertices) or nodes and directed E (dges) or arrows. Using a $G([V][E])$ notation, we base the definition of $G = T_{\geq 0}$ (Fig.1b, Def.3) on *iterations* of the just defined upward and rightward functions U_0 and R_0 (Defs.1-2) that generate its upward and rightward arrows $[E]$ and the implied congruence classes of its upward and rightward node subsets $[V]$. Iterations U_0^j and R_0^k of the upward and rightward function, denoted by superscripts j and k , give to each rightward argument an upward path of upward successors $s_{\geq 1} \rightarrow S_1 \rightarrow S_2 \rightarrow S_3 \rightarrow \dots$ and to each upward argument a rightward path of rightward successors $S_{\geq 1} \rightarrow s_1 \rightarrow s_2 \rightarrow s_3 \rightarrow \dots$ (Fig.1b, Def. 3).

$$T_{\geq 0} \left(\begin{array}{c} [c5, c27]_{288} \\ [U_0, R_0] \end{array} \right) = \left(\begin{array}{c} U_0^j: s_{\geq 0} \rightarrow S_j, \text{ for } j = 1, 2, 3, \dots \text{ (Fig. 1b, upward paths, blue)} \\ R_0^k: s_0 \rightarrow s_0, S_{\geq 1} \rightarrow s_k \text{ for } k = 1, 2, 3, \dots \text{ (rightward paths, red)} \end{array} \right) \quad (3)$$

with $S_{\geq 0} = [4, 16]_{18} = [c5, c27]_{288}$; $S_{\geq 1} = [c5]_{288}$; $s_{\geq 0} = [c27]_{288}$;

$S_{\geq 0}$ includes $S_{\geq 1}$ and $s_{\geq 0}$; $s_{\geq 0}$ includes s_0 and $s_{\geq 1}$; s_0 holds the root $\Omega_{\geq 0} = 4$;

$S_{\geq 1}$ includes S_1, S_2, S_3, \dots ; $s_{\geq 1}$ includes s_1, s_2, s_3, \dots .

Fig.2 does not by itself exclude trees rooted in, for example, a diverging trajectory from infinity downwards to a colossally high lowest number reached by $[16]_{18} \rightleftharpoons [17]_{18}$ cycles that amount to $(n-1)/3 \cdot 2^1 = 2/3n - 1/3$ contractions per cycle. Based on Definition 3, the sought-for proof that all branching numbers $S_{\geq 0} = [4, 16]_{18}$ and, hence, all numbers \mathbb{N} (Fig.2), are fully contained in tree $T_{\geq 0}$ with root subset s_0 holding the cyclic root $4 \rightarrow 2 \rightarrow 1 \rightarrow 4$ (Fig.1-2) can be broken down into a proof on the successor subsets S_1, S_2, S_3, \dots , and s_1, s_2, s_3, \dots (Fig1b, Def. 4).

3 Automorphism graph of subtrees and cotrees

For a proof on the successor subsets S_1, S_2, S_3, \dots and s_1, s_2, s_3, \dots , each of which is scattered across the entire tree $T_{\geq 0}$ (Fig. 1b), the tree graph must be reconfigured, as in the paper on hypergraphs by Collatz [12] or in De Bruijn graphs facilitating genome assembly.[13] We align the scattered numbers of distinct successor subsets in disjoint cotrees T_1, T_2, T_3, \dots and t_1, t_2, t_3, \dots (Fig. 4), in which they inherit one-to-one the nodes, inner arrows and root paths of their own ancestors in tree

$T_{\geq 0}$. The subtrees and cotrees are themselves nodes in a directed automorphism graph, labelled $\text{Aut}(T_{\geq 0}, U_0, R_0)$, with paths from the binary tree $T_{\geq 0}$ mapping nodes and arrows one-to-one to them defined by iterates and conjugates of the leftward and rightward functions (Def. 4, Fig.5).

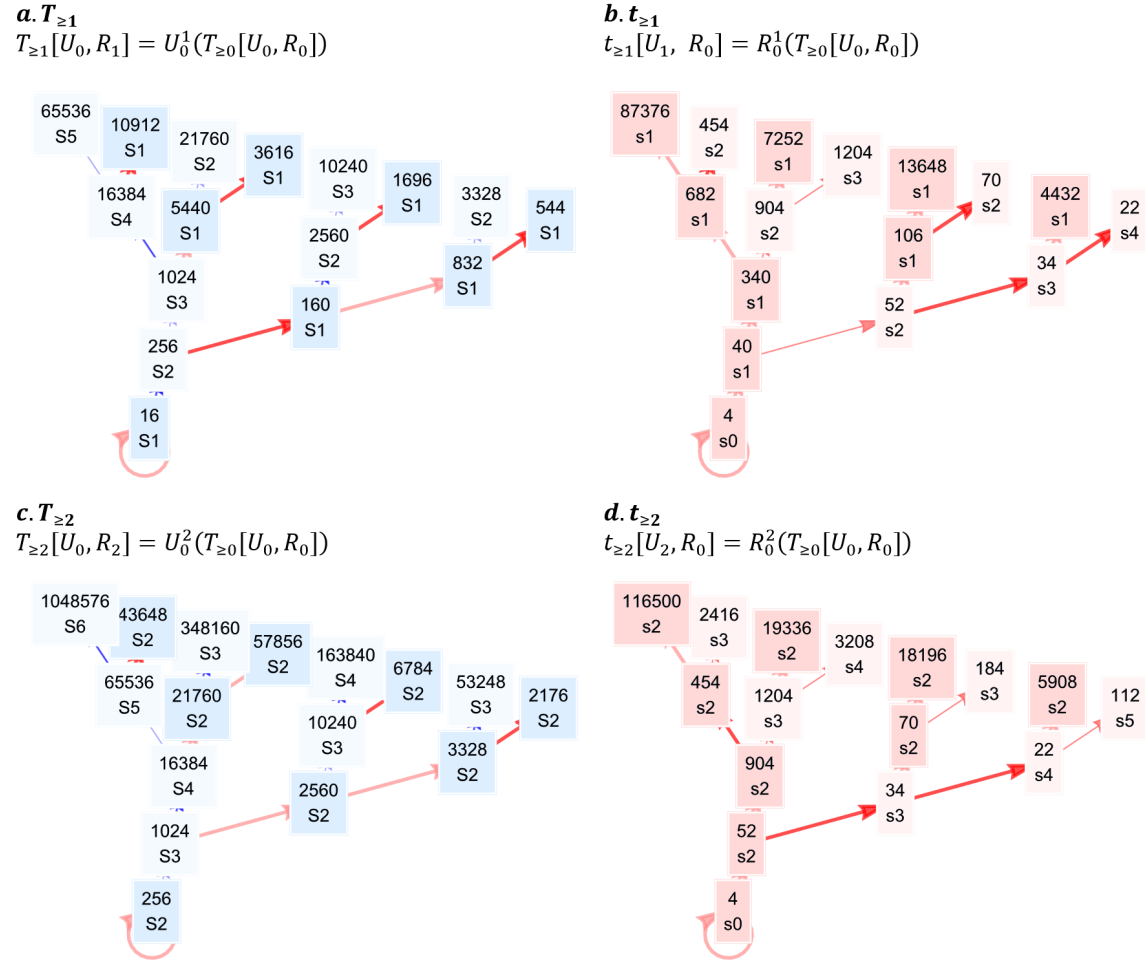


Fig. 3 | Exemplars upward subtrees $T_{\geq 1}, T_{\geq 2}, \dots$ and rightward subtrees $t_{\geq 1}, t_{\geq 2}, \dots$ (a) $S_{\geq 1}$ paths $160_{S1} \rightarrow 2560_{S2} \rightarrow 10240_{S3} \rightarrow \dots$ in tree $T_{\geq 1}$, (c) $S_{\geq 2}$ paths $2560_{S2} \rightarrow 10240_{S3} \rightarrow \dots$ in tree $T_{\geq 2}$, and so on, align with the path of a rightward ancestor in tree $T_{\geq 0}$ having upward successors $40_{S1} \rightarrow 160_{S1} \rightarrow 2560_{S2} \rightarrow 10240_{S3} \rightarrow \dots$ (Fig.1b). Analogously, (b) $s_{\geq 1}$ paths $340_{S1} \rightarrow 904_{S2} \rightarrow 1204_{S3} \rightarrow \dots$ in $t_{\geq 1}$, (d) $s_{\geq 2}$ paths $904_{S2} \rightarrow 1204_{S3} \rightarrow \dots$ in tree $t_{\geq 2}$, and so on, align with the path of an upward ancestor in tree $T_{\geq 0}$ having rightward successors $256_{S2} \rightarrow 340_{S1} \rightarrow 904_{S2} \rightarrow 1204_{S3} \rightarrow \dots$ (Fig.1b).

Rightward R_0 arrows, for example, $40_{S1} \rightarrow 52_{S2}$, with end node successors $52_{S2} \rightarrow 832_{S1} \rightarrow 3328_{S2} \rightarrow \dots$ in tree $T_{\geq 0}$ (Fig.1b) become conjugate R_j arrows (a) $160_{S1} \rightarrow 832_{S1}$ in $T_{\geq 1}$, (c) $2560_{S2} \rightarrow 3328_{S2}$ in tree $T_{\geq 2}$ and so on. Upward U_0 arrows, for example, $256_{S2} \rightarrow 1024_{S3}$, with end node successors $1024_{S3} \rightarrow 682_{S1} \rightarrow 454_{S2} \rightarrow \dots$ in tree $T_{\geq 0}$ (Fig.1b), become conjugate U_k arrows (b) $340_{S1} \rightarrow 682_{S1}$ in tree $t_{\geq 1}$, (d) $904_{S2} \rightarrow 454_{S2}$ in tree $t_{\geq 2}$ and so on. |

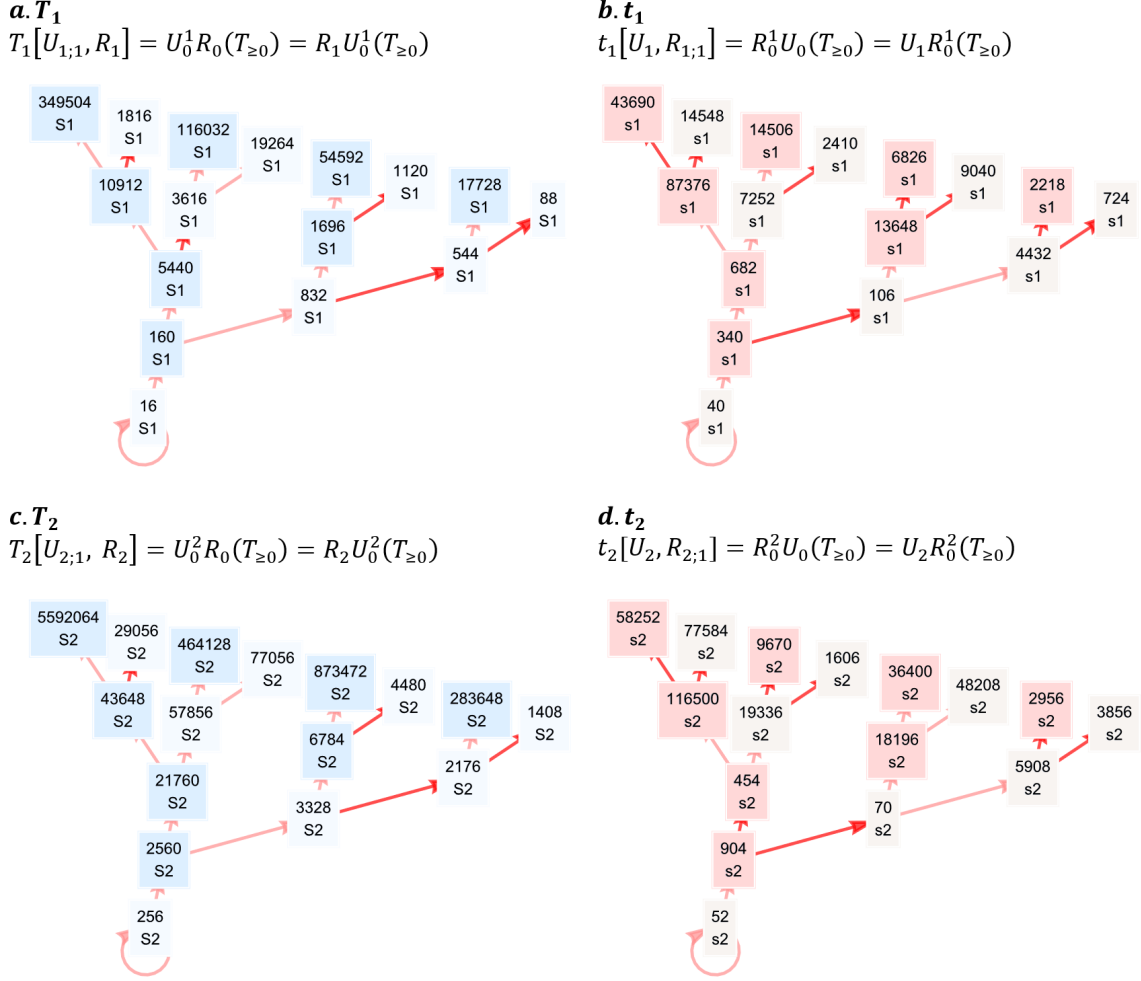


Fig. 4 | Exemplars upward cotrees T_1, T_2, \dots and rightward cotrees t_1, t_2, \dots (a) Upward cotree $T_1 = R_1(T_{\geq 1})$ removes $S_{>1}$ ancestor 1024_{S_3} from the R_1 path $1024_{S_3} \rightarrow 5440_{S_1} \rightarrow 3616_{S_1} \rightarrow \dots$ in $1024_{S_3} \rightarrow 5440_{S_1} \rightarrow 3616_{S_1} \rightarrow \dots$ subtree $T_{\geq 1}$ (Fig.3a). (c) $T_2 = R_2(T_{\geq 2})$ removes $S_{>2}$ ancestor 16384_{S_4} from R_2 path $16384_{S_4} \rightarrow 21760_{S_2} \rightarrow 57856_{S_2} \rightarrow \dots$ in $T_{\geq 2}$ (Fig.3c). Analogously, (b) rightward cotree $t_1 = U_1(t_{\geq 1})$ removes $s_{>1}$ ancestor 52_{s_2} from the conjugate upward U_1 path $52_{s_2} \rightarrow 106_{s_1} \rightarrow 13648_{s_1} \rightarrow \dots$ in subtree $t_{\geq 1}$ (Fig.3b). (d) $t_2 = U_2(t_{\geq 2})$ removes $s_{>2}$ ancestor 34_{s_3} from U_2 path $34_{s_3} \rightarrow 70_{s_2} \rightarrow 18196_{s_2} \rightarrow \dots$ in $t_{\geq 2}$ (Fig.3d).

The conjugate upward arrows in upward cotrees follow from upward arrows in tree $T_{\geq 0}$. See, for example, how $U_0 : 16_{S_1} \rightarrow 256_{S_2}$ (Fig.1b) having paired successors $16_{S_1} \rightarrow 40_{s_1} \rightarrow 160_{S_1} \rightarrow 2560_{S_2} \rightarrow \dots$ and $256_{S_2} \rightarrow 340_{s_1} \rightarrow 5440_{S_1} \rightarrow 21760_{S_2} \rightarrow \dots$ (Fig.2) yields (a) $U_{1;1} : 160_{S_1} \rightarrow 5440_{S_1}$ in cotree T_1 and (c) $U_{2;1} : 2560_{S_2} \rightarrow 21760_{S_2}$ in cotree T_2 . Analogously, conjugate rightward arrows in rightward cotrees follow from rightward arrows in $T_{\geq 0}$. |

3.1 Outer paths yield subtrees

Subfigures 3a-c illustrate that subtree aligning iterations $T_{\geq j} = U_0^j(T_{\geq 0})$ for $j = 1, 2, 3, \dots$ align paths of rightward ancestors with upward successors $s_{\geq 1} \rightarrow S_1 \rightarrow S_2 \rightarrow S_3 \rightarrow \dots$ in tree $T_{\geq 0}$ (Fig.1b) with upward $S_{\geq j}$ paths $S_j \rightarrow S_{j+1} \rightarrow S_{j+2} \rightarrow \dots$ in tree $T_{\geq j}$. Analogously, subfigures 3b-d illustrate that iterations of the rightward function $t_{\geq j} = R_0^k(T_{\geq 0})$ for $k = 1, 2, 3, \dots$ align paths of upward ancestors with rightward successors $S_{\geq 1} \rightarrow s_1 \rightarrow s_2 \rightarrow s_3 \rightarrow \dots$ in tree $T_{\geq 0}$ (Fig.1b) with rightward $s_{\geq k}$ paths $s_k \rightarrow s_{k+1} \rightarrow s_{k+2} \rightarrow \dots$ in tree $t_{\geq k}$.

The strange fact that infinite subsets of numbers $s_{\geq 1}, S_1, S_2, \dots, S_{j-1}$ and $S_{\geq 1}, s_1, s_2, \dots, s_{k-1}$ can be excluded from infinite paths, with a number remaining at each node, was exemplified by David Hilbert (1862–1943) with a fully booked infinite hotel[14] that remains full despite guests leaving. An infinite number of remaining guests are available to move into the empty rooms below them. The greater-or-equal notation for dual modules (Doppelmoduln) of nested series (of sets of congruence classes) dates back at least to Emmy Noether (1882-1935)[15, 16]

Once a generation of successors takes the ancestor nodes, the ancestor arrows are transformed into *conjugate inner arrows*. Conjugate arrows are defined by the U -shaped function $f_i = g^i f_0 g^{-i}$, referred to as the inner automorphism function,[16] the pair-of-pairs-function, rotation quaternions, versors or, after Max Dehn (1878–1952) in 1911, the transformation function,[17] with conjugates (default 0, no conjugation) in subscript and iterates (default 1, first iteration) in superscript. Rightward R_0 arrows $s_{\geq 1x} \rightarrow s_{\geq 1y}$, which pair two paths of rightward ancestors having upward successors $s_{\geq 1x} \rightarrow S_{1x} \rightarrow S_{2x} \rightarrow \dots \rightarrow S_{jx} \rightarrow \dots$ and $s_{\geq 1y} \rightarrow S_{1y} \rightarrow S_{2y} \rightarrow \dots \rightarrow S_{jy} \rightarrow \dots$ in tree $T_{\geq 0}$, yield conjugate rightward R_j arrows $S_{jx} \rightarrow S_{jy}$ in subtree $T_{\geq j}$, defined as $R_j = U_0^j R_0 U_0^{-j}$ (Fig.3ac). Analogously, upward U_0 arrows $S_{\geq 1x} \rightarrow S_{\geq 1y}$, which pair two paths of upward ancestors having rightward successors, yield conjugate upward U_k arrows $s_{kx} \rightarrow s_{ky}$ in subtree $t_{\geq k}$, defined as $U_k = R_0^k U_0 R_0^{-k}$ (Fig.3bd). Using square brackets to denote functions that generate inner arrows, we obtain upward subtrees $T_{\geq j}[U_0, R_j] = U_0^j(T_{\geq 0}[U_0, R_0])$ with nodes $S_{\geq j}$ and rightward subtrees $t_{\geq k}[U_k, R_0] = R_0^k(T_{\geq 0}[R_0, U_0])$ with nodes $s_{\geq k}$ (Def.4, Fig.5).

3.2 Outer paths yield disjoint cotrees

Comparing subfigures 4ac with 3ac reveals that rightward S_j paths starting from upward $S_{> j}$ ancestors $S_{> j} \rightarrow S_{j1} \rightarrow S_{j2} \rightarrow \dots$ in subtree $T_{\geq j}$, align with exclusive S_j paths $S_{j1} \rightarrow S_{j2} \rightarrow \dots$ of conjugate R_j arrows in cotree T_j . Analogously, subfigures 4bd and 3bd illustrate that upward s_k paths starting from rightward $s_{> k}$ ancestors $s_{> k} \rightarrow s_{k1} \rightarrow s_{k2} \rightarrow \dots$ in subtree $t_{\geq k}$, align with exclusive s_k paths $s_{k1} \rightarrow s_{k2} \rightarrow \dots$ of conjugate U_k arrows in cotree t_k .

The inner upward arrows in upward cotree T_j follow from the definition of the conjugacy function $T_j = R_j U_0^j(T_{\geq 0}) = U_0^j R_0 U_0^{-j} U_0^j(T_{\geq 0}) = U_0^j R_0(T_{\geq 0})$. Upward arrows $S_{\geq 1x} \rightarrow S_{\geq 1y}$ in tree $T_{\geq 0}$, with paired upward paths $S_{\geq 1x} \rightarrow s_{\geq 1x} \rightarrow S_{1x} \rightarrow S_{2x} \rightarrow \dots \rightarrow S_{jx} \rightarrow \dots$ and $S_{\geq 1y} \rightarrow s_{\geq 1y} \rightarrow S_{1y} \rightarrow S_{2y} \rightarrow \dots \rightarrow S_{jy} \rightarrow \dots$, yield double conjugate upward arrows $S_{jx} \rightarrow S_{jy}$ (Figs. 3a-c, 4a-c), defined as $U_{j;1} = U^j(R_0^1 U_0 R_0^{-1}) U^{-j}$ in cotree $T_j[U_{j;1}, R_j] = R_j(T_{\geq j}[U_0, R_j]) = R_j U_0^j(T_{\geq 0}[U_0, R_0])$. Analogously, rightward arrows in tree $T_{\geq 0}$ yield double conjugate inner rightward arrows $R_{k;1} = R^k(U_0^1 R_0 U_0^{-1}) R^{-k}$ in rightward cotree $t_k[U_{k;1}, R_k] = U_k(t_{\geq j}[U_k, R_0]) = U_k R_0^k(T_{\geq 0}[U_0, R_0])$ (Def. 4, Fig.5).

3.3 Defining the automorphism graph

Definition 5 captures the outer arrows—denoted as prefix functions—and the inner arrows—denoted within square brackets—of the automorphism graph $\text{Aut}(T_{\geq 0}, U_0, R_0)$.

$$\begin{array}{ll}
 \text{Argument root tree:} & T_{\geq 0}[U_0, R_0] \\
 \text{Upward subtrees:} & T_{\geq j} = U_0^j(T_{\geq 0}) \text{ yields } T_{\geq j}[U_0, R_j] \\
 \text{Upward cotrees:} & T_j = U_0^j R_0^1(T_{\geq 0}) = R_1 U_0^j(T_{\geq 0}) \text{ yields } T_j[U_{j;1}, R_j] \\
 \text{Rightward subtrees:} & t_{\geq k} = R_0^k(T_{\geq 0}) \text{ yields } t_{\geq k}[U_k, R_0] \\
 \text{Rightward cotrees:} & t_k = R_0^k U_0^1(T_{\geq 0}) = U_1 R_0^k(T_{\geq 0}) \text{ yields } t_k[U_k, R_{k;1}] \\
 \text{Identity non-moves:} & U_0^0, R_0^0, U_j^0, R_k^0 \\
 \text{Conjugate functions:} & R_j = U_0^j R_0 U_0^{-j} \qquad U_k = R_0^k U_0 R_0^{-k}, \\
 & U_{j;1} = U^j (R_0^1 U_0 R_0^{-1}) U^{-j} \qquad R_{k;1} = R^k (U_0^1 R_0 U_0^{-1}) R^{-k}
 \end{array} \tag{4}$$

The automorphism graph $\text{Aut}(T_{\geq 0}, U_0, R_0)$ is a version of the automorphism group of any infinite binary tree, also with respect to conjugate functions.[18, 19] However, Definition 6 takes numerical Collatz labels *at* the nodes of $T_{\geq 0}$, rather than combinations of a 0,1-alphabet to denote the nodes themselves.[18, 19]

The iterated functions and the conjugated functions each form a group since they are themselves invertible (e.g., $U_0^i U_0^{-i} = U_0^0$), additive ($U_0^i U_0^j = U_0^{i+j}$ in the domain $i + j \geq 0$), associative ($U_0^i (U_0^j U_0^k) = (U_0^i U_0^j) U_0^k = U_0^{i+j+k}$) and commutative ($U_0^i U_0^j = U_0^j U_0^i$). As with any tree, the reversal of upward and rightward moves is *non-commutative* ($U_0^j R_0 \neq R_0 U_0^j$). *Conjugates* allow for reversal after all ($R_j U_0^j = U_0^j R_0 U_0^{-j} U_0^j = U_0^j R_0$, $U_k R_0^k = R_0^k U_0 R_0^{-k} R_0^k = R_0^k U_0$), which also proves that cotrees can be defined with two paths, one of them providing a second conjugate root path in a disjoint cotree.

Infinite recursion is allowed, but not required here. Applying the cotree generating outer arrow functions $U_0^j R_0^1$ and $R_0^k U_0^1$ to an output cotree generates two infinite series of disjoint cotrees within that cotree.

3.4 Depicting the automorphism graph

In Fig. 5, the automorphism graph $\text{Aut}(T_{\geq 0}, U_0, R_0)$ is depicted as a directed, butterfly-shaped graph with two infinite wings: one of upward subtrees and cotrees and one with rightward subtrees and cotrees. The *butterfly lemma* is a later label for the Zassenhaus lemma,[20] which is an isomorphism lemma[15, 16] in a butterfly-shaped quotient group of congruence classes with finite wings.[21] Graphs with trees as nodes are fairly uncommon, but see [22].

Fig.5 includes the congruence classes of five trees whose densities - denoted with the Greek rho - and cotree density decay factors recur in propositions 5, 6 and 7. Specifications for all subtrees and cotrees are included in the Ancillary Materials (Method, Extended Definition 4).

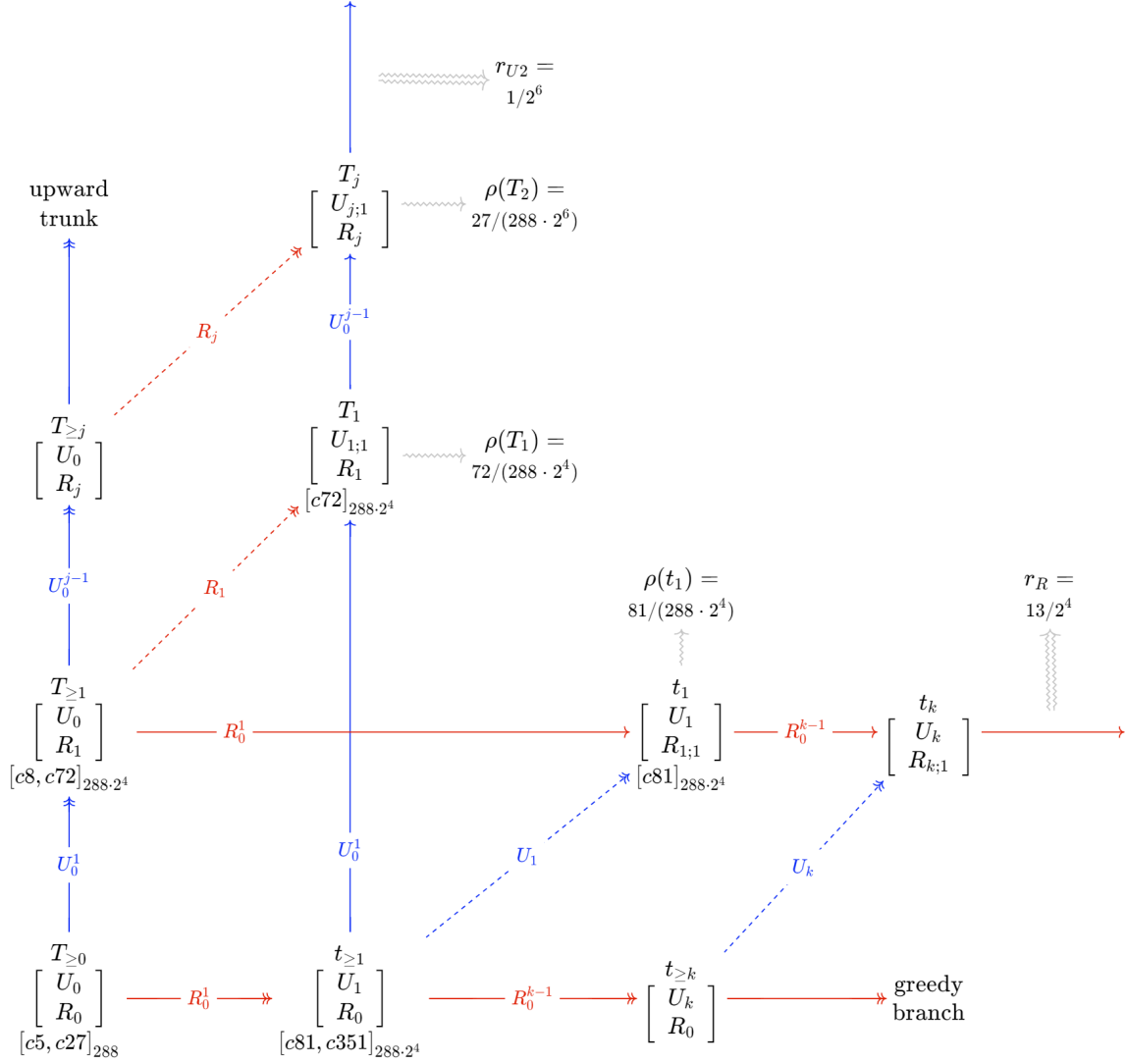


Fig. 5 | Automorphism graph $\text{Aut}(T_{\geq 0}, U_0, R_0)$ Arrows vs. brackets: outer vs. inner automorphism. Blue vs. red arrows: upward vs. rightward tree generation. Single vs. double arrowheads (\rightarrow vs. \rightarrow or \triangleright): cotree vs subtree generation. Uppercase vs. lowercase subtrees (T vs. t): upward vs rightward trees. Superscript vs. subscript, solid vs. dashed arrows: iterations vs. conjugations, with iterations U_0^j, R_0^k and conjugations $R_j, U_k, U_{j;1}, R_{k;1}$. Table 1 enumerates the sets of congruence classes $c5, c27, c8, c72, c81, c351$ of trees $T_{\geq 0}, T_{\geq 1}, t_{\geq 1}, T_1, t_1$. Propositions 5, 6 and 7 concerning geometric sums of cotree densities $s = a/(1-r)$ rest on the cotree densities $\rho(T_1), \rho(T_1), \rho(t_1)$ and the cotree density decay factors R_{U_2}, R_R . |

Table 1 | Base sets of congruence classes subtrees and cotrees

$u2 = [4,16]_{18}$, branching numbers $[S_{\geq 0}]_{18}$, alignment by $\vec{h}_U = [4,1]$
 $r6 = [4,16,22,34,40,52]_{54}$, branching numbers $[S_{\geq 0}]_{54}$, alignment by $\vec{h}_R = [4,2,1,8,4,8]$

c5, upward numbers in $T_{\geq 0}[c5,c27]_{288}$, count by $u2$: $c5\#u2 = [1,4]$
 $[[16,88,160,232][256]]$

c27, rightward numbers in $T_{\geq 0}[c5,c27]_{288}$, count by $u2$: $c5\#u2 = [15,12]$,
 $[[4,22,40,58,76,94,112,130,148,166,184,202,220,238,274],$
 $[34,52,70,106,124,142,178,196,214,250,268,286]]$

3c5, rightward arguments $[3c5]_{288.3}$, count by $r6$: $3c5\#r6 = [1,4,1,4,1,4]$
 $[[544], [16,232,448,664], [832], [88,304,520,736], [256], [160,376,592,808]]$

3c27, rightward arguments $[3c27]_{288.3}$, count by $r6$: $3c27\#r6 = [15,12,15,12,15,12]$ (not listed)

c72, in $T_{\geq 1}[c8,c72]_{288.2^4}$ and in $T_1[c72]_{288.2^4}$, count by $u2$: $c72\#u2 = [12,60]$
 $[[544,832,1120,1696,1984,2272,2848,3136,3424,4000,4288,4576],$
 $[16,88,160,232,304,376,448,520,592,664,736,808,880,952,1096,1168,1240,1312,1384,1456,1528,1600,1672,$
 $1744,1816,1888,1960,2032,2104,2248,2320,2392,2464,2536,2608,2680,2752,2824,2896,2968,3040,3112,3184,$
 $3256,3400,3472,3544,3616,3688,3760,3832,3904,3976,4048,4120,4192,4264,4336,4408,4552]]$

c8, in $T_{\geq 1}[c8,c72]_{288.2^4}$, count by $u2$: $c8\#u2 = [4,4]$
 $[[256,1408,2560,3712], [1024,2176,3328,4480]]$

c81, in $t_{\geq 1}[c81,c351]_{288.2^4}$ and in $t_1[c81]_{288.2^4}$,
3c81, rightward argument period, count by $r6$: $3c81\#r6 = [3(15,12,15,12,15,12)]$ ($c81\#r6$ listed)
 $[[58,490,922,1192,1354,1786,2218,2650,2920,3028,3082,3514,3946,4378,4432],$
 $[340,394,826,1258,1690,2122,2554,2986,3418,3796,3850,4282],$
 $[346,616,724,778,1210,1642,2074,2344,2506,2938,3370,3802,4072,4180,4234],$
 $[250,682,1114,1492,1546,1978,2410,2842,3274,3706,4138,4570],$
 $[40,202,634,1066,1498,1768,1876,1930,2362,2794,3226,3496,3658,4090,4522],$
 $[106,538,970,1402,1834,2266,2644,2698,3130,3562,3994,4426]]$

c351, in $t_{\geq 1}[c81,c351]_{288.2^4}$
3c351, rightward arguments, count by $r6$: $3c351\#r6 = [13(15,12,15,12,15,12)]$ ($c351\#r6$ listed)
 $[[4,112,166,220,274,328,382,436,598,652,706,760,814,868,976,1030,1084,1138,1246,1300,1462,1516,1570,$
 $1624,1678,1732,1840,1894,1948,2002,2056,2110,2164,2326,2380,2434,2488,2542,2596,2704,2758,2812,2866,$
 $2974,3190,3244,3298,3352,3406,3460,3568,3622,3676,3730,3784,3838,3892,4054,4108,4162,4216,4270,4324,$
 $4486,4540,4594], [70,124,178,286,502,556,610,718,772,934,988,1042,1150,1204,1366,1420,1474,1582,1636,$
 $1798,1852,1906,2014,2068,2230,2284,2338,2446,2500,2662,2716,2770,2878,2932,3094,3148,3202,3310,3364,$
 $3526,3580,3634,3742,3958,4012,4066,4174,4228,4390,4444,4498,4606], [22,76,130,184,238,292,400,454,$
 $508,562,670,886,940,994,1048,1102,1156,1264,1318,1372,1426,1480,1534,1588,1750,1804,1858,1912,1966,$
 $2020,2128,2182,2236,2290,2398,2452,2614,2668,2722,2776,2830,2884,2992,3046,3100,3154,3208,3262,3316,$
 $3478,3532,3586,3640,3694,3748,3856,3910,3964,4018,4126,4342,4396,4450,4504,4558], [34,142,196,358,$
 $412,466,574,628,790,844,898,1006,1060,1222,1276,1330,1438,1654,1708,1762,1870,1924,2086,2140,2194,$
 $2302,2356,2518,2572,2626,2734,2788,2950,3004,3058,3166,3220,3382,3436,3490,3598,3652,3814,3868,3922,$
 $4030,4084,4246,4300,4354,4462,4516], [94,148,310,364,418,472,526,580,688,742,796,850,904,958,1012,$
 $1174,1228,1282,1336,1390,1444,1552,1606,1660,1714,1822,2038,2092,2146,2200,2254,2308,2416,2470,2524,$
 $2578,2632,2686,2740,2902,2956,3010,3064,3118,3172,3280,3334,3388,3442,3550,3604,3766,3820,3874,3928,$
 $3982,4036,4144,4198,4252,4306,4360,4414,4468], [52,214,268,322,430,484,646,700,754,862,916,1078,1132,$
 $1186,1294,1348,1510,1564,1618,1726,1780,1942,1996,2050,2158,2212,2374,2428,2482,2590,2806,2860,2914,$
 $3022,3076,3238,3292,3346,3454,3508,3670,3724,3778,3886,3940,4102,4156,4210,4318,4372,4534,4588]]$

4 Cumulative cotree densities

Definitions of paths of outer arrows towards cotrees $T_j = R_j U_0^j(T_{\geq 0})$ and $t_k = U_k R_0^k(T_{\geq 0})$ (Def. 4, Fig.5) also determine their congruence classes and periodicities. Cotree density is obtained by dividing the number of cotree congruence classes by their periodicity, thus the density of the two classes $[4, 16]_{18}$ with periodicity 18 is indeed $2/18$. Propositions 5, 6 and 7 express the cumulative densities of even upward cotrees, odd upward cotrees and rightward cotrees as geometric series $s = a/(1 - r)$. As shown in Fig.5, the nominator a regards the densities of their first exemplars $\rho(T_2)$, $\rho(T_1)$ and $\rho(t_1)$, respectively, while r represents cotree density decay, dependent on the periodicity expansion factors $\theta_{U_2} = 2^6$, $\theta_{U_1} = 2^4$ and $3\theta_R = 2^4$ (Defs.1,2). This cotree density proof is a variant on the density proof based on node subsets removed from a binary Collatz tree of odd numbers $[1, 5]_6$, in which the correspondence between removed subsets and the node sets of cotrees in the automorphism graph of the binary tree was implicit.[23]

A placeholder box notation $[\square, \square]_{\square}$ is used in propositions 5, 6 and 7 to indicate of which cotree the still unspecified sets of congruence classes and their periodicity will be determined, while = ... highlights missing links yet to be filled in.

$$\begin{aligned}
 T_2[\square, \square]_{\square} &= R_2 U_0^2(T_{\geq 0}[c5, c27]_{288}) = \dots & (5) \\
 &= R_2(T_{\geq 2}[(c5, c27) \cdot 2^6]_{288 \cdot 2^6}) = T_2[c27 \cdot 2^6]_{288 \cdot 2^6} \\
 \text{density } \rho(T_2) &= 27/(288 \cdot 2^6), \text{ density decay } r_{U_2} = 1/\theta_{U_2} = 1/2^6, \\
 \text{density even upward cotrees } \rho(T_2, T_4, T_6, \dots) &= \rho(T_2)/(1 - r_{U_2}) = 1/672
 \end{aligned}$$

The missing link in (5) is resolved by the 2^6 higher periodicity $\theta_{U_2} = 2^6$ and the 2^6 times higher congruence classes $U_0^2(n) = 2^6 n$ after two upward iterations (Def.1), yielding a density decay of $1/\theta_{U_2} = 1/2^6$. For example, since $[40]_{288}$ is one of the $c27$ congruence classes in $T_{\geq 0}$, $[40 \cdot 2^6]_{288 \cdot 2^6} = [2560]_{18432}$ is one of the 27 congruence classes in T_2 .

$$\begin{aligned}
 T_1[\square, \square]_{\square} &= R_1 U_0^1(T_{\geq 0}[c5, c27]_{288}) = \dots & (6) \\
 &= R_1(T_{\geq 1}[c8, c72]_{288 \cdot 2^4}) = T_1[c72]_{288 \cdot 2^4}, \\
 \text{density } \rho(T_1) &= 72/(288 \cdot 2^4), \text{ density decay } r_{U_2} = 1/\theta_{U_2} = 1/2^6 \\
 \text{density odd upward cotrees } \rho(T_1, T_3, T_5, \dots) &= \rho(T_1)/(1 - r_{U_2}) = 1/63
 \end{aligned}$$

The missing link in (6) can be filled in via the upward expansion factor $\theta_{U_1} = 2^4$ (Fig. 2, Def. 1), which expands the upward output periodicity from 288 to $288\theta_{U_1} = 4608$. Because the upward periodicity alignment vector $\vec{h}_{U_1} = [4, 1]$ is conditional on arguments $u_2 = [4, 16]_{18}$ (Def.1), the output congruence classes with periodicity $288\theta_{U_1}$ are conditional on partitions of the argument classes $[c5]_{288}$ and $[c27]_{288}$ into $c5[1, 4]_{\#u_2}$ and $c27[15, 12]_{\#u_2}$, respectively, which can be verified with Table 1. Table 1 enumerates the resulting upward sets $c8$ of $1 \cdot 4 + 4 \cdot 1 = 8$ and $c72$ of $15 \cdot 4 + 12 \cdot 1 = 72$ congruence classes of the first upward subtree $T_{\geq 1}[c8, c72]_{288 \cdot 2^4}$. Odd upward cotrees have 72 congruence classes with density decay $r_{U_2} = 1/\theta_{U_2} = 1/2^6$. For example, if $[88]_{288 \cdot 2^4}$ is a

$c72$ congruence class in T_1 , then $[88 \cdot 2^6]_{288 \cdot 2^{4+6}} = [5632]_{294912}$ is one of the 72 congruence classes in T_3 .

$$\begin{aligned} t_1[\square, \square]_{\square} &= U_1 R_0^1(T_{\geq 0}[c5, c27]_{288}) = U_1 R_0^1(T_{\geq 0}[3c5, 3c27]_{288 \cdot 3}) = \dots \\ &= U_1(t_{\geq 1}[3c81, 3c351]_{288 \cdot 3 \cdot 3}) = t_1[c81]_{288 \cdot 2^4}, \end{aligned} \quad (7)$$

$$\text{density } \rho(t_1) = 81/(288 \cdot 2^4), \text{ density decay } r_R = \dots = 13/(3\theta_R) = 13/2^4$$

$$\text{density rightward cotrees } \rho(t_1, t_2, t_3, \dots) = \rho(t_1)/(1 - r_R) = 27/288$$

The missing link in (7) is filled by rightward output expansions by $3\theta_R = 16$, starting from a triple-expanded argument period (Fig. 2, Def. 2). Because the rightward alignment vector $\vec{h}_R[4, 2, 1, 8, 4, 8]$ is conditional on $r6 = [4, 16, 22, 34, 40, 52]_{54}$, rightward output congruence classes are conditional on the partitions of the expanded argument classes $[3c5]_{288 \cdot 3}$ and $[3c27]_{288 \cdot 3}$ into $3c5[1, 4, 1, 4, 1, 4]_{\#r6}$ and $3c27[15, 12, 15, 12, 15, 12]_{\#r6}$, respectively (Table 1). The resulting rightward sets $c81$ of $1 \cdot 4 + 4 \cdot 2 + \dots + 4 \cdot 8 = 81$ and $c351$ of $15 \cdot 4 + 12 \cdot 4 + \dots + 12 \cdot 8 = 351$ congruence classes of the first rightward subtree $t_{\geq 1}[c81, c351]_{288 \cdot 2^4}$ are listed in Table 1.

Unlike the congruence classes of even and odd upward subtrees, those of rightward subtrees $t_{\geq k}$ cannot be simplified to one geometric series. Their *set sizes* build a geometric series because each triple-expanded argument subclass results in three different argument subclasses at the next iteration, as indicated by the transformation matrix T (Fig. 2; Ancillary Fig. 3, Def. 4). Multiplication with $\vec{h}_R[4, 2, 1, 8, 4, 8]$ and matrix multiplication with T at each rightward iteration turns the set sizes $[1, 4, 1, 4, 1, 4]_{\#r6}$ and $[15, 12, 15, 12, 15, 12]_{\#r6}$ of the sets $[3c5]_{288 \cdot 3}$ and $[3c27]_{288 \cdot 3}$, respectively, in tree $T_{\geq 0}$ into triple-expanded set sizes $[3 \cdot 13^{k-1}(15, 12, 15, 15, 12)]_{\#r6}$ and $[3 \cdot 13^{k-1}(69, 48, 69, 48, 69, 48)]_{\#r6}$, respectively, of any rightward subtree $t_{\geq k}$. The rightward density decay is therefore $13/(3\theta_R) = 13/2^4$.

Figure 2 showed that the numbers from 16 congruence classes modulo 18 that do not branch in two directions are connected by the Collatz function to the set $S_{\geq 0} = [4, 16]_{18}$ of branching numbers with density $2/18$. The proof of proposition 8 that the cumulative densities of numbers in disjoint cotrees of tree $T_{\geq 0}$ from propositions 5, 6 and 7 add up to $2/18$ indeed, is therefore also proof that all branching numbers in set $S_{\geq 0}$ with density $2/18$ are nodes in subtree $T_{\geq 0}$ of T_C , and that all numbers from the set of natural numbers \mathbb{N} with density $2/18 + 16/18 = 1$ are nodes in the Collatz tree T_C .

$$\begin{aligned} \text{Density binary tree } \rho(T_{\geq 0}) & \quad (8) \\ &= \rho(\text{upward cotrees } T_1, T_2, T_3, \dots) + \rho(\text{rightward cotrees } t_1, t_2, t_3, \dots) \\ &= (1/63 + 1/672) + 27/288 \\ &= 5/288 + 27/288 = 2/18 \end{aligned}$$

Thus, the Collatz tree includes all natural numbers, which proves the Collatz conjecture. Isolated trajectories do not exist. The greedy branch OEIS A225570 is rightly called *greedy*[2] as $27/32$ of the branching numbers are based in it rather than in the upward trunk.

5 Discussion

As anticipated by its proposer [1], our proof of the Collatz conjecture was substantially facilitated by connecting elementary number and elementary graph theory. Congruence classes from elementary number theory applied to cotrees in the directed automorphism graph of the binary Collatz tree enabled our proof that all natural numbers are included in the Collatz tree.

The binary Collatz tree suggests many cross-cutting connections. Its numbers have two successors, while the 'number line' elicits one successor. Each number has a unique binary root path of *upward* or *rightward* steps (Fig. 1b: $160 \rightarrow 1, 0, 1$). This decomposition is curiously reminiscent of prime factorisation, which maps each number to a unique sequence of powers of successive primes ($160 \rightarrow 2^5 \cdot 3^0 \cdot 5 = 5, 0, 1$). The automorphism graph (Fig.5) comprises many remarkable numbers, such as its base periodicity 288 (two gross), 1,2,3,c5,c8,13 (Fibonacci numbers)[24], $c72+c81=c153$ cotree congruence classes that generate all generations of branching numbers (miraculous fish catch) and $13 \cdot c27=c351$ nested rightward congruence classes (number of computable functions by one of 4,096 Turing machines with 2 states and 2 colours).[25]

The unary functions generating the automorphism group of the Collatz tree may have counterparts in modelling graph replications[26, 27] in quantum physics, human learning, cell biology and/or social networking. The Collatz automorphism graph may be helpful in other avenues already explored by Collatz sequences, such as pseudo-random number generation,[28] encryption[29, 30] and watermarking[31] - digital elements of our daily lives that are becoming increasingly important.

Ancillary Materials |

- SupplementAutCollatzTree.pdf: supplementary Figures, extended Definition 4, acknowledgments (9 pp.)
- Math12AutCollatzTree.nb: Mathematica notebook, our functions to define, depict and explore the Collatz tree
- Math12AutCollatzTree.pdf: landscape pdf-print Mathematica notebook (91 pp.)

Works [32, 33, 34, 35, 36] from the references below are quoted in the ancillary materials.

References

- [1] L. Collatz, *On the motivation and origin of the $(3n + 1)$ -problem*, pp. 241–248. Providence, Rhode Island: American Mathematical Society, 2010.
- [2] E. Roosendaal, *On the $3x + 1$ problem*. <http://www.ericr.nl/wondrous/>, Last update at the time of writing: March 22, 2022.
- [3] D. Barina, “Convergence verification of the Collatz problem,” *The Journal of Supercomputing*, vol. 77, no. 3, pp. 2681–2688, 2021.
- [4] J. C. Lagarias, *The Ultimate Challenge: The $3x + 1$ Problem*. Rhode Island: AMS Bookstore, 2010.
- [5] OEIS Inc, *The Online Encyclopedia of Integer Sequences*. <https://oeis.org>.
- [6] M. Chamberland, *A $3x + 1$ survey: Number Theory and dynamical systems*, pp. 57–78. Providence, Rhode Island: American Mathematical Society, 2010.
- [7] T. Tao, “Almost all orbits of the Collatz map attain almost bounded values,” *arXiv*, vol. 1909.03562, 2019.
- [8] A. V. Kontorovich and J. C. Lagarias, *Stochastic models for the $3x+1$ and $5x+1$ problems and related problems*, pp. 131–188. Providence, Rhode Island: AMS, 2010.
- [9] Veritasium, *The Simplest Math Problem No One Can Solve - Collatz Conjecture, interview with A.V. Kontorovich*. <https://www.youtube.com/watch?v=094y1Z2wpJg>, 2021.
- [10] J. C. Lagarias, A. M. Odlyzko, and J. B. Shearer, “On the density of sequences of integers the sum of no two of which is a square,” *Journal of Combinatorial Theory, Series A*, vol. 33, no. 2, pp. 167–185, 1982.
- [11] M. H. Weissman, *An illustrated theory of numbers*. Providence: American Mathematical Society, 2017.
- [12] L. Collatz, *Verzweigungsdiagramme und Hypergraphen*, pp. 9–42. Springer, 1977.
- [13] P. E. C. Compeau, P. A. Pevzner, and G. Tesler, “How to apply de Bruijn graphs to genome assembly,” *Nature Biotechnology*, vol. 29, no. 11, pp. 987–991, 2011.
- [14] D. Hilbert, *Über das Unendliche*, pp. 730–731. Heidelberg: Springer, 1924.
- [15] E. Noether, “Hyperkomplexe Grössen und Darstellungstheorien,” *Mathematische Zeitschrift*, vol. 30, pp. 641–692, 1929.
- [16] E. Noether and W. Schmeidler, “Moduln in nichtkommutativen Bereichen,” *Mathematische Zeitschrift*, vol. 8, pp. 1–35, 1920.
- [17] M. Dehn, “Über unendliche diskontinuierliche Gruppen,” *Mathematische Annalen*, vol. 71, no. 1, pp. 116–144, 1911.
- [18] A. M. Brunner and S. Sidki, “On the automorphism group of the one-rooted binary tree,” *Journal of Algebra*, vol. 195, no. 2, pp. 465–486, 1997.
- [19] B. E. Nucinkis and S. S. John-Green, “Quasi-automorphisms of the infinite rooted 2-edge-coloured binary tree,” *Groups, Geometry, and Dynamics*, vol. 12, no. 2, pp. 529–570, 2018.
- [20] H. Zassenhaus, “Zum Satz von Jordan-Hölder-Schreier,” *Abhandlungen aus dem Mathematischen Seminar der Universität Hamburg*, vol. 10, no. 1, pp. 106–108, 1934.
- [21] J. B. Fraleigh, *A first course in abstract algebra*. Pearson Education India, 2003.
- [22] C. Lu, J. X. Yu, Z. Zhang, and H. Cheng, *Graph Iso/Auto-Morphism: A Divide and Conquer Approach*, p. 1195–1207. New York, NY, USA: Association for Computing Machinery, 2021.

- [23] J. Kleinnijenhuis, A. M. Kleinnijenhuis, and M. G. Aydogan, *The Collatz tree as a Hilbert hotel*. <https://arxiv.org/abs/2008.13643v1>, 31 Aug 2020, 2020.
- [24] M. Albert, B. Gudmundsson, and H. Ulfarsson, “Collatz meets Fibonacci,” *Mathematics Magazine*, pp. 1–7, 2022.
- [25] S. Wolfram, *A new kind of Science*. Wolfram Inc., 2001.
- [26] D. L. Barabási and D. Czégel, “Constructing graphs from genetic encodings,” *Scientific Reports*, vol. 11, no. 1, pp. 1–13, 2021.
- [27] D. V. Lakshmi and L. Jeganathan, “Graph self-replication system,” *Complex Systems*, vol. 28, no. 3, 2019.
- [28] D. Xu, “Pseudo-random number generators based on the Collatz conjecture,” *International Journal of Information Technology*, vol. 11, no. 3, p. 453, 2019.
- [29] D. Renza, “High-uncertainty audio signal encryption based on the Collatz conjecture,” *Journal of Information Security and Applications*, vol. 46, p. 62, 2019.
- [30] A. Gupta, I. J. Aberkane, S. Ghosh, A. Abold, A. Rahn, and E. Sultanow, “Rotating binaries,” *Applied-Math*, vol. 2, no. 1, pp. 104–117, 2022.
- [31] H. Ma, C. Jia, S. Li, W. Zheng, and D. Wu, “Xmark: dynamic software watermarking using the Collatz conjecture,” *IEEE Transactions on Information Forensics and Security*, vol. 14, no. 11, pp. 2859–2874, 2019.
- [32] K. Andersson, *On the boundedness of Collatz sequences*. <https://arxiv.org/abs/1403.7425>, 2014.
- [33] Frogfanitw, “<http://math.stackexchange.com/questions/1571469/collatz-modulo-18-partitions-of-collatz-3n1-trajectories>,” 2015.
- [34] E. Sultanow, C. Koch, and S. Cox, *Collatz Sequences in the Light of Graph Theory*. <https://doi.org/10.25932/publishup-43008>, <https://github.com/c4ristian/collatz>, 2020.
- [35] D. R. Hofstadter, *Gödel, Escher, Bach: an eternal golden braid*. New York: Basic Books, 1980.
- [36] S. Wolfram, *Mathematica: a system for doing mathematics by computer*. Addison Wesley Longman Publishing Co., Inc., 1991.